

Article

Thermal Behavior and Morphology of Thermoplastic Polyurethane Derived from Different Chain Extenders of 1,3- and 1,4-Butanediol

Chia-Fang Lee ¹, Chin-Wen Chen ^{1,*} , Syang-Peng Rwei ^{1,*}  and Fu-Sheng Chuang ²

¹ Research and Development Center for Smart Textile Technology, Institute of Organic and Polymeric Materials, National Taipei University of Technology, Taipei 10608, Taiwan; t9519006@ntut.edu.tw

² Department of Fashion and Design, Lee-Ming Institute of Technology, No. 22, Sec. 3, Tai-Lin Rd., Taishan Dist., New Taipei City 243, Taiwan; ymj0826@mail.lit.edu.tw

* Correspondence: cwchen@ntut.edu.tw (C.-W.C.); f10714@ntut.edu.tw (S.-P.R.)

Abstract: In this study, when deriving thermoplastic polyurethane (TPU), the researchers replaced 1,4-butanediol (1,4-BDO) with 1,3-butanediol (1,3-BDO) as a chain extender and examined how the structure of the chain extender affected the final polymers. Regarding the raw materials for polymerization, three types of commercial polyols with the same molecular weight ($M_n = 1000$ g/mol), namely, poly (butyl acrylate) (PBA), poly (tetramethylene ether) glycol (PTMG), and polycarbonate diol (PCDL) were used. These polyols were used in conjunction with butanediol and 4,4'-methylene diphenyl diisocyanate. Three groups of TPUs were successfully synthesized using one-shot solvent-free bulk polymerization. Compared with TPUs polymerized using 1,4-BDO, materials polymerized using 1,3-BDO are more transparent and viscous. Structural analysis revealed that no substantial differences between the final structures of the TPUs were present when different chain extenders were used. Thermal analysis indicated that compared with TPUs polymerized using 1,4-BDO, the glass transition temperature of those with 1,3-BDO was 15 °C higher. Examination of microphase separation in the structure by using morphological analysis revealed that compared with TPUs synthesized using 1,4-BDO, PBA, and PTMG synthesized using 1,3-BDO were relatively separated. PCDL synthesized using 1,3-BDO exhibited no morphological difference. Rheological analysis indicated PCDL synthesized using either 1,4-BDO or 1,3-BDO did not exhibit any obvious differences. In conclusion, TPUs synthesized using PCDL and 1,3-BDO exhibited thermal plasticity at room temperature (15–20 °C). Their basic application could be extended to the development of smart materials. In terms of further application, they could be used in shape memory and temperature-sensitive high molecular polymers.

Keywords: thermoplastic polyurethane; chain extender; thermal behavior; morphology; microphase separation; rheology



Citation: Lee, C.-F.; Chen, C.-W.; Rwei, S.-P.; Chuang, F.-S. Thermal Behavior and Morphology of Thermoplastic Polyurethane Derived from Different Chain Extenders of 1,3- and 1,4-Butanediol. *Appl. Sci.* **2021**, *11*, 698. <https://doi.org/10.3390/app11020698>

Received: 29 November 2020

Accepted: 10 January 2021

Published: 13 January 2021

Publisher's Note: MDPI stays neutral with regard to jurisdictional claims in published maps and institutional affiliations.



Copyright: © 2021 by the authors. Licensee MDPI, Basel, Switzerland. This article is an open access article distributed under the terms and conditions of the Creative Commons Attribution (CC BY) license (<https://creativecommons.org/licenses/by/4.0/>).

1. Introduction

Among the rapid advancements in smart high polymer materials, the innovation of thermoplastic polyurethanes (TPUs) is a key area [1–3]. Compared with polyurethane (PU), TPU is a type of high polymer elastomer material. Specifically, it is a type of thermoplastic elastomer (TPE). In recent years, the amount of research related to TPUs has increased substantially. TPU is composed of hard to soft rubbery polymers; it has excellent abrasion resistance, is tough, and is oil and solvent resistant. Additionally, it possesses characteristics such as high elasticity, high tensile strength, and high ductility. Recent research directions in developing TPU are related to the polymer structure. The structure of TPU is a main block copolymer, which is made up of alternating soft and hard chain segments that endow the materials with softness and rigidity, respectively. The polymerization of TPU involves three constituents, namely isocyanate, polyol (i.e., macrodiol), and the diol

that acts as the chain extender. The hard chain segment is composed of isocyanate and the chain extender, whereas polyalcohol is the main structure of the soft chain segment. Currently, the polyols commonly used in the TPU market are polyether and polyester, but both types of polyols have application limitations. Only recently did polycarbonate become the new generation of polyols. Because the polycarbonate functional group has a high level of polarity and a strong intermolecular force, strong and tough mechanical performance could be achieved with the use of polycarbonate [4]. It offers good resistance to hydrolytics and oxidation, so polycarbonate could also be an excellent candidate for the biostability polymer [5]. Hence, new discoveries were made from the transition of CO₂ into polycarbonate due to the awareness of greenhouse gas [6]. Wang and co-workers showed that waterborne polyurethane from CO₂-polyol may achieve better hydrolysis resistance than poly (butyl acrylate) (PBA) [7]. Although the cost associated with polycarbonate is relatively high [8,9], the number of relevant studies has increased markedly in recent years. Application problems have been solved based on the constituents of the polymers, and this could be extended to the development of new types of high molecular polymers.

TPU is a type of block copolymer. The thermal incompatibility between the chain segments is a crucial factor affecting the structure. The miscibility of TPU affects the microphase separation of the structure, including the transition temperature from a glassy state to a rubbery state and the formation of hard and soft zones through modification of soft and hard chain segments. Many researchers have investigated the influence of the constituents and the contents of the hard chain segments on TPU [10–12]; the constituent structure is also extensively used in material science applications. The rubber-like form of TPU can be used to achieve the shape memory effect. By manipulating the constituents of soft and hard chain segments, TPU with an amorphous reversible phase may cause shape memory [13–17]. In the past decades, considerable attention has been focused on smart high polymer materials on shape memory [14,15], which is also applicable in smart textile products [18].

One point worth noting is that the recent research has focused on isocyanate; it is believed to be the main influence in the formation of hard zones [19], soft zones [20], and the soft/hard zone structure ratio [21]. Using a chain extender could enhance the glass-transition temperature (T_g) and elastic modulus by changing the hard/soft segment interrelation [22]. Without using a chain extender, polyurethanes reacted by isocyanates and macrodiols were lacking physical properties and microphase separation [23]. However, few studies have actually discussed the influence of the chain extender on the chain segment. In the TPU industry, 1,4-BDO is often used as a chain extender; its straight chain structure is beneficial for forming long chain linear block copolymers. However, according to toxicity data in the TOXNET of the National Library of Medicine on the National Institutes of Health campus in the United States, the toxicity of 1,4-BDO is much greater than that of 1,3-BDO [24]. Additionally, inhaling hazards may occur during the polymerization process; Lora-Tamayo et al. reported a poisoning case caused by 1,4-BDO. Usage of 1,4-BDO may not be entirely safe [25]. With regard to research on chain extenders, researchers have used different types of short chain diols in the polymerization reaction [26,27]; some have used 1,3-BDO in the polymerization to examine its further application as an alternative use to 1,4-BDO and may have an additional benefit for industrial usage, i.e., modulating the glass-transition temperature to room temperature. Additionally, Zhang's study indicated that the short side chain could be used in regulating the glass-transition temperature and bio-based shape memory PU [28]. Although an enormous amount of research has already been conducted on the key factors that affect the hard/soft zone of isocyanates, research into using butanediol as the chain extender is relatively rare. In recent years, understanding of butanediol has deepened, and research on bio-based short chain diols has already been conducted in different fields [29–31]. Using the fermentation process to catalyze the reaction, biobased butanediol could be created [32]. To understand the mechanisms behind it, the current study attempted to examine how the chain extender could influence the structure of TPU [33–41].

In the field of TPU research, the microphase separation of hard and soft chains is a topic worth exploring. The morphology of the microphase would affect the final performance of TPU [42–44]. Some researchers have discussed the influence of the ratio of hard chain segments and soft chain segments on phase separation [45,46]. Niemczyk and co-workers proposed that a hydrogen bond would crystallize with TPU partially [47]; thus, the soft chain segment could be used to establish the elastic modulus and flexible characteristics by affecting the cross-linking density of polyurethane [22]. Xiao discovered that adding different soft chain segments to the PU elastomer would significantly change its material properties [48]. Studies conducted in recent years have chosen to produce TPU by using different structures, and these studies could be applied in adhesive additives [49–54]. Researchers have conducted studies on diols to distinguish their bonding properties. Using a fixed NCO/OH ratio, Mónica used polypropylene glycols with different molecular weights to prepare TPU pressure-sensitive adhesive [55]; this study highlighted the centrality of hard chain segment content and also confirmed that TPU could be used as an adhesive [56]. Wamuo also stressed the importance of the chain structure to the crystal, and the set speed of hot melt glue could be confirmed [57]. The results of other studies conducted in recent years have indicated that rheological properties could be used to evaluate complex materials similar to TPU. The viscoelastic properties of adhesives are essential with regard to adhesive performance; additionally, the balance between their elasticity (solid state) and viscosity (liquid state) could help researchers in understanding their properties. Additionally, when rheological methods are used to examine the shear thinning and frequency scanning and to examine their viscoelasticity, the results could be used in confirming whether materials could be candidate adhesives (e.g., hot melt glue or pressure-sensitive adhesive).

Based on the foregoing literature review, the researchers in the current study replaced 1,4-BDO with 1,3-BDO in the synthesis of TPUs and examined the thermal, morphological, and rheological effects. The research was aimed to gain an understanding of the production of TPUs from this perspective, with the hope of understanding the possibility of applying it in smart materials. Specifically, the researchers wished to confirm whether materials with unique properties could be produced using a new direction, with findings useful in developing new types of high polymer material.

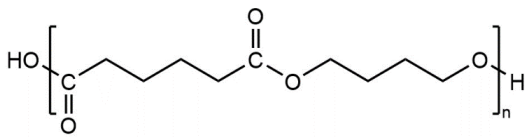
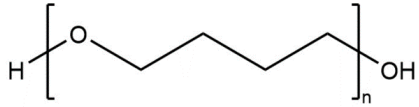
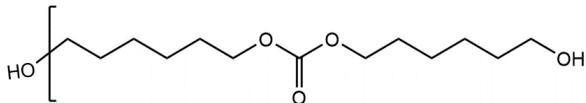
2. Materials and Methods

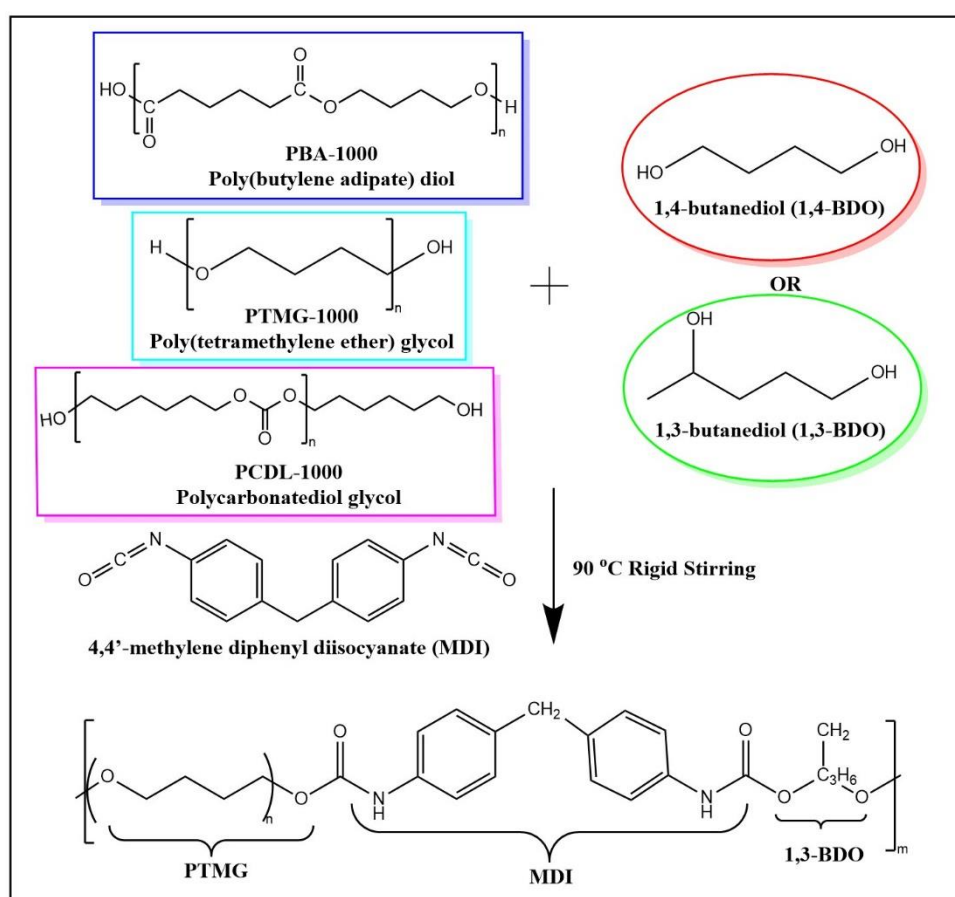
2.1. Materials

Three types of polyol were used in synthesizing TPUs. The researchers performed grouping based on structure and performed detailed experimental comparisons. The three function groups were polyester, polyether, and polycarbonate. Poly (butylene adipate) diol (PBA) is a linear polyester polyol (Lydye Chemical, $M_n = 1000$ g/mol). Poly (tetramethylene ether) glycol (PTMG) is a type of linear polyether (Lydye Chemical, $M_n = 1000$ g/mol), and polycarbonate diol (PCDL) is a type of carbonate polyol (Tosho NIPPOLLAN 981, $M_n = 1000$ g/mol). Their structural differences could be used to achieve different performances in the PU/TPU industry. The structures of the three types of polyol are provided in Table 1.

For a polymerization flow diagram of the TPUs, refer to Scheme 1. Three types of polyols and chain extender were used to prepare six types of TPUs. The final polymer product in the diagram is the polymerization product of PTMG and 1,3-BDO.

Table 1. The types of polyol used in synthesizing thermoplastic polyurethanes (TPUs).

Polyols	Abbreviation	Chemical Structure of the Main Components
Poly(butylene adipate) diol	PBA	
Poly(tetramethylene ether) glycol	PTMG	
Polycarbonatediol	PCDL	



Scheme 1. Synthesis flow of TPUs using different chain extenders. Three types of polyol (PBA, PTMG, PCDL; $M_n = 1000$ g/mol) and 1,4-butanediol (1,4-BDO) or 1,3-butanediol (1,3-BDO) and 4,4'-methylene diphenyl diisocyanate (MDI) were used to prepare a series of TPUs. The final polymer product shown in the flow diagram has the structure of TPU block copolymers composed of PTMG and 1,3-BDO.

Regarding the hard chain section of the TPUs, 1,4-butanediol (Alfa Aesar, Ward Hill, MA, USA) and 1,3-butanediol (Alfa Aesar, Ward Hill, MA, USA) were used. The aromatic diisocyanate 4,4'-diphenylmethane diisocyanate (MDI) used originated from BASF, of Germany. All the materials were used immediately after they were received. Each TPU formula used the same mole ratio, and the NCO/OH of the hard chain segment is R. To control the influence

of hard chain segment on the TPUs, we designed two compounding ratios, $R = 1.00$ and $R = 1.02$; this was done to determine whether the increase of hard chain segments would affect structure and performance. For the constituents of the two hard chain segments, see Table 2.

Table 2. Formula structures and $[NCO]/[OH]$ ratios of thermoplastic polyurethanes.

MDI: Polyols: BDO (Molar Ratio)	$[NCO]/[OH]$ (R Value)	Hard Segment (wt %)
2:1:1	1.00	37.13
2.02:1:1	1.02	37.52

2.2. Synthesis of Thermoplastic Polyurethanes (TPUs)

In this experiment, the researchers used a one-shot solvent-free bulk polymerization to synthesize TPUs. First, three types of polyol and chain extenders were placed in a vacuum oven. They were heated at $80\text{ }^{\circ}\text{C}$ for 4 h to remove moisture. For the MDI, they were placed in a $60\text{ }^{\circ}\text{C}$ oven for 2 h to convert them to a solution state. The polymerization reaction could be started after all the materials were prepared.

First, the polyol and the chain extender were placed in an acrylic plaster beaker, and a polyol-BDO premixed solution was prepared by mixing the ingredients thoroughly using a mixer. Next, MDI was added to the premixed solution, and they underwent a homogeneous reaction in a short amount of time. After the reaction was completed, the reactants were placed on a board smeared with polytetrafluoroethylene, and then they were placed in an oven at $120\text{ }^{\circ}\text{C}$ for 3 h of consolidation. The final product was a piece of TPU material to be used for experimentation.

2.3. Preparation of TPU Films

To investigate the properties of the TPUs, the researchers prepared thin films for thermal and morphological analysis using the solvent casting method. The TPU block materials were dissolved around 30–40 wt % in N-dimethylacetamide solution, then poured on a glass pane, and baked for 20 h to form thin films casting.

The coding of the TPU materials in the current study are explained as follows: the first part of the sign is related to the polyol, whereas the second part is related to the chain extender used. For example, “PCDL-1,3-BDO” means that during the synthesizing process, PCDL was the choice of polyol, and 1,3-BDO was the chain extender. Two types of hard chain indices were designed for each group of TPU formula to discuss the influence of hard chain segment on TPU. The $[NCO]/[OH]$ ratio is set as the R value. The third part of the formula sign consists of the R value. For example, “PBA-1,4-R = 1.02” means PBA was used as the polyol and 1,4-BDO as the chain extender during the synthesizing process, with the hard chain index R value being 1.02. This formula was used to conduct the synthesizing process, and the codes are used to display the research results.

2.4. Instrumental Methods

2.4.1. Fourier Transform Infrared Spectrometry (FT-IR)

To express the chemical structure of the TPUs, 16 scans were performed with a Perkin Elmer Spotlight 200i Sp2 equipped with an AutoATR system. The scope of data collected using the transmission mode was $4000\text{--}400\text{ cm}^{-1}$, and the resolution ratio was 4 cm^{-1} .

2.4.2. Gel Permeation Chromatography (GPC)

After the TPUs were synthesized, their molecular weight was confirmed through gel permeation chromatography (GPC) using a Viscotek GPCmax VE-2001. The number-average molecular weight (M_n), weight-average molecular weight (M_w), and polydispersity index (PDI) were examined using GPC. The mobile phase featured a 1 mL min^{-1} current velocity using dimethylformamide (DMF) under $60\text{ }^{\circ}\text{C}$; the column was $300\text{ mm} \times 810\text{ mm}$.

2.4.3. Thermogravimetric Analysis (TGA)

Thermal stability was investigated through thermogravimetric analysis (TGA). The samples were heated from 35 °C to 500 °C in N₂ air by using NETZSCH TG 209 F3 with a temperature rate of 10 °C/min; the variations in the sample weight according to the increase in temperature were recorded.

2.4.4. Differential Scanning Calorimetry (DSC)

For measurement of thermal performance, glass transition temperature (T_g), and melting temperature (T_m), the differential scanning calorimetry (DSC) method was used; the measurements were taken using a HITACHI SIINT SII X-DSC7000 instrument. First, 4–8 mg of each sample were sealed in an aluminum pan, placed on the platform, and maintained at the system-maintained temperature of –60 °C for 10 min. Next, the samples were heated to 220 °C at a temperature rate of 10 °C/min. After this heating process was maintained for 3 min, a cooling scan from 220 to –60 °C was performed at a cooling rate of –10 °C/min. The temperature rising and cooling scans of the samples were performed under a nitrogen gas condition; T_m and T_g values were obtained from the second scan.

2.4.5. Dynamic Mechanical Analysis (DMA)

The researchers performed a dynamic mechanical analysis (DMA) using HITACHI DMS 6100. With regard to the testing method, a stretching mode with 0.5% dynamic stretch was used, and the specimen dimensions were controlled between 40 mm (length) × 10 mm (width); the thickness of the specimen was maintained between 0.2 and 0.3 mm. The DMA system temperature was set from –60 °C to 110 °C, and the heating rate was 5 °C/min; the frequency used was 1 Hz.

2.4.6. Atomic Force Microscope (AFM)

With regard to morphological analysis for investigating microphase separation, an atomic force microscope (AFM) was used to understand the conditions of the hard and soft chain segments. The researchers used Park XE-100 to perform surface analysis of the sample thin films at room temperature and the scanning scope was 10 μm × 10 μm and 5 μm × 5 μm, respectively. A microscope was used to observe and capture the morphology of the surface. TPU samples subjected to three annealing time lengths (0, 10, and 20 h) were scanned; the annealing time was used to understand the degree of microphase separation.

2.4.7. Rheological Measurement

Rheological measurements were taken using an Anton Paar Physica MCR Rheometer using two rheological methods. The samples were placed on a 1 mm gap and heated to 200 °C. Then, the samples were tested using steady shear flow and dynamic oscillatory flow. In the steady shear flow experiments, the shear rate was set to 0.1–100 1/s for the observation of rheological behaviors under shear thinning. The purpose of using the oscillatory flow was to collect data related to the storage modulus (G') and the loss modulus (G'') as well as to confirm the condition of the melt viscosity. The oscillatory experiment was conducted in the frequency range of 0.01 to 100 Hz with strain = 5% at 200 °C to determine whether the deformation was proportional to the stress and whether the deformation indicated the physical significance of the viscoelastic modulus.

3. Results and Discussion

In this study, the researchers used the one-shot solvent-free bulk polymerization method to synthesize polyol, MDI, and BDO into TPU. Because 1,3-BDO was used in place of 1,4-BDO as a chain extender, FT-IR analysis had to be used to confirm any changes in the structure of the TPUs. FT-IR spectrum diagrams of TPUs with three different functional groups are displayed in Figure 1. A stretching and bended vibration-NH absorption band is present at the 3330 cm⁻¹ point; this is a characteristic of a carbamate functional group. The vibration band present at the 2730 cm⁻¹ point has a N=C=O structure; these representations

of absorption peaks also indicate a carbamate functional group. These results indicate that TPU was successfully synthesized using both 1,3-BDO and 1,4-BDO as the chain extender with varying polyols.

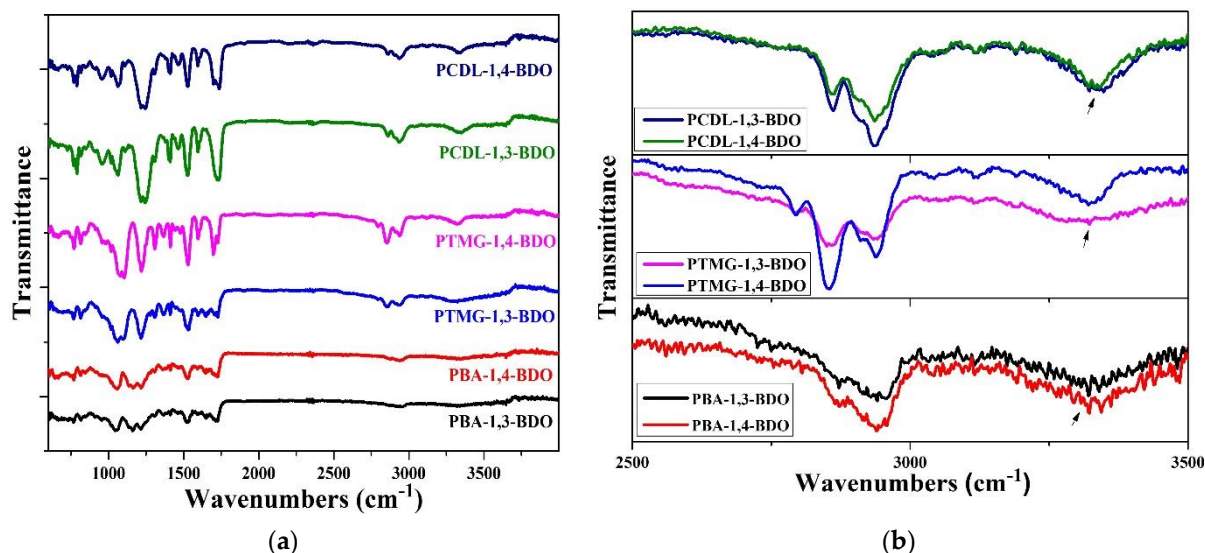


Figure 1. Fourier transform infrared (FT-IR) light spectrum diagram of the three groups of TPU, synthesized using different polyols (PBA, PTMG, or PCDL) and different chain extenders. (a) full graph and (b) graph between 2500 to 3500 cm^{-1} . (the arrow is located in 3300 cm^{-1}).

The number-average molecular weight (M_n), weight-average molecular weight (M_w), and polydispersity index (PDI), according to the molecular distribution data obtained from the GPC analysis, are listed in Table 3. The results revealed that even when 1,4-BDO was replaced by 1,3-BDO, TPU with high molecular weight could be polymerized. The PDI values of all the TPU samples were lower than 2.0; this means that this method is applicable in terms of polymer processing (e.g., injection molding and extrusion) [13]. Next, thermal analysis and testing were conducted to confirm the structure. Examination of the thermal properties was performed to gain further understanding of the TPUs for application and research.

Table 3. Number-average molecular weight (M_n), weight-average molecular weight (M_w), and polydispersity index (PDI) of the TPUs synthesized in this study.

Polymer Code	M_n (g/mol)	M_w (g/mol)	M_w/M_n (PDI)
PBA-1,3-R = 1	106,553	160,281	1.50
PBA-1,3-R = 1.02	109,180	184,483	1.69
PBA-1,4-R = 1	153,223	274,070	1.79
PBA-1,4-R = 1.02	141,036	208,916	1.48
PCDL-1,3-R = 1	126,288	198,902	1.58
PCDL-1,3-R = 1.02	82,993	150,089	1.81
PCDL-1,4-R = 1	187,687	356,779	1.90
PCDL-1,4-R = 1.02	94,794	151,253	1.60
PTMG-1,3-R = 1	114,117	163,701	1.43
PTMG-1,3-R = 1.02	108,948	162,242	1.49
PTMG-1,4-R = 1	96,633	142,240	1.47
PTMG-1,4-R = 1.02	109,293	183,788	1.68

TGA was used to evaluate thermal stability during the thermal degradation process. Figure 2 illustrates the thermal degradation conditions of TPU under inert gas; the figure indicates that even when different chain extenders were used during the polymerization

process, the thermal degradation temperatures of the TPUs were similar (approximately 300 °C). For PBA and PTMG groups, the TGA spectra indicate a two-stage thermal degradation [58], and this involves the degradation of the hard and the soft chain segments [59]. The first stage of degradation is related to carbonate bonds, whereas the second stage originates from the polyol structure. However, only one peak was observed for the PCDL group; this is probably because the PCDL group has a higher level of phase mixture; thus, the two-stage degradation is less obvious [60]. With regard to the degradation temperature (T_d), when the weight loss was 5%, the T_d of the TPU polymerized using 1,3-BDO was 2–5 °C lower than the T_d of the TPU polymerized using 1,4-BDO. The reason behind this is probably that the methyl bonds of 1,3-BDO can be damaged more easily under high temperature, and this resulted in a relatively lower thermal degradation temperature. However, regardless of the type of butanediol used, the thermal degradation spectra of the TPUs are similar. The use of 1,3-BDO as the chain extender did not greatly affect the polymer structure, indicating that the polymerized TPUs have excellent thermal stability.

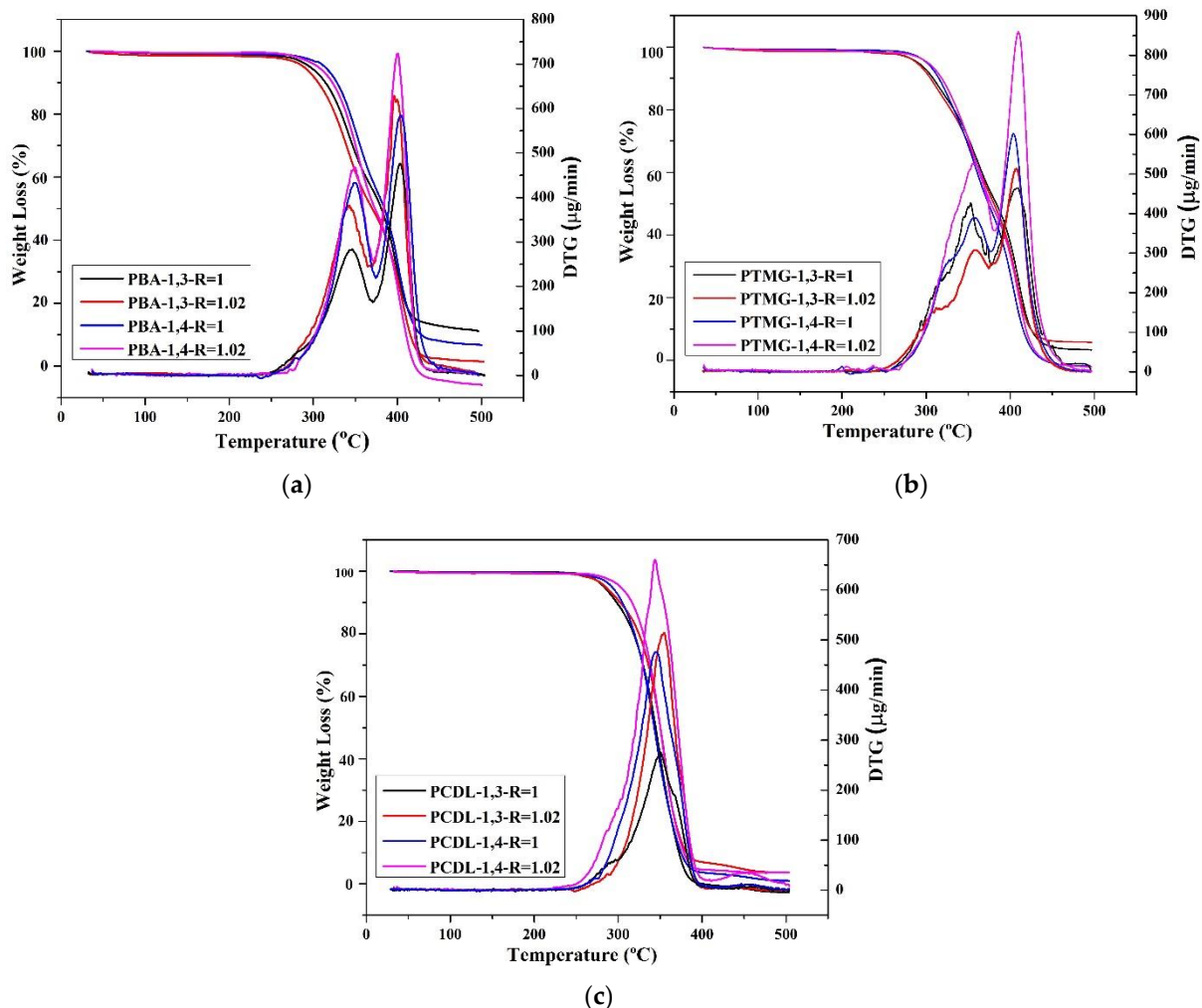


Figure 2. Thermogravimetric analysis (TGA) and differential thermogravimetry (DTG) spectra of TPU prepared through the polymerization of PBA (a), PTMG (b), or PCDL (c), with 1,3-BDO or 1,4-BDO.

The thermal conversion effect was evaluated using DSC. The thermal properties of the TPUs are presented in Figure 3, which clearly illustrates that the TPUs synthesized using 1,3-BDO have no temperature for melting (T_m). For TPUs synthesized using 1,4-BD, their T_m range is between 139 °C and 150 °C; this is common for TPUs. The TPUs synthesized using 1,3-BDO also have no melting point; this indicates that their structures are not crystalline, and this is related to the fact that they possess some viscosity.

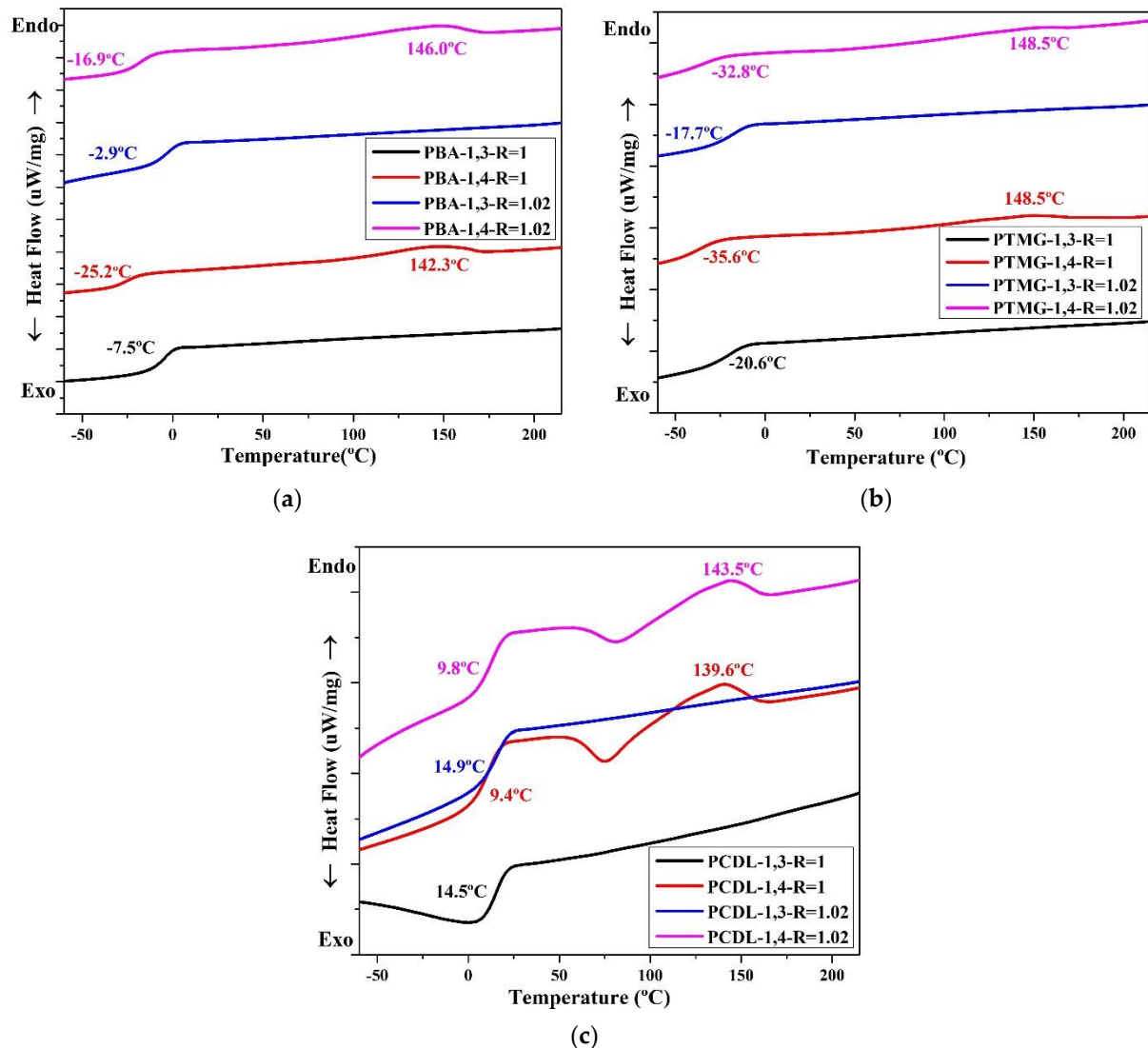


Figure 3. Differential scanning calorimetry (DSC) thermograms of TPU formed through the polymerization of PBA (a), PTMG (b), or PCDL (c), with 1,3-BDO or 1,4-BDO.

When 1,3-BDO was used as the chain extender in synthesizing TPU, the glass transition temperature (T_g) was higher than when synthesis was performed with 1,4-BDO. When two types of polyol, namely PBA or PTMG, are used in synthesizing TPU, the T_g of TPU synthesized using 1,3-BDO was approximately 10–15 °C higher than the T_g of TPU synthesized using 1,4-BDO. When PCDL was used to synthesize TPU, the T_g of the TPU synthesized using 1,3-BDO was approximately 5 °C higher than that of the TPU synthesized using 1,4-BDO. The results also revealed the T_g of TPU synthesized from PCDL and 1,3-BDO was approximately 15 °C; this temperature is close to room temperature (15–25 °C) [28,61]. This indicates that the TPU could be used as a novel type of composite material produced through high polymer processing at room temperature (20 °C) [16].

The researchers compared the major mechanical characteristics (storage modulus (G'), loss modulus (G''), and $\tan \delta$) using DMA. According to the data (Figure 4), the $\tan \delta$ values of TPU synthesized using 1,3-BDO are higher than the $\tan \delta$ values of TPU synthesized using 1,4-BDO. This confirms that when 1,3-BDO was used for the synthesis, the appearance of the resultant TPU was soft and viscous. Based on the storage modulus diagram, the storage modulus of TPU synthesized using 1,4-BDO would be significantly

reduced under lower temperature than TPU synthesized using 1,3-BDO; this is probably related to their lower T_g .

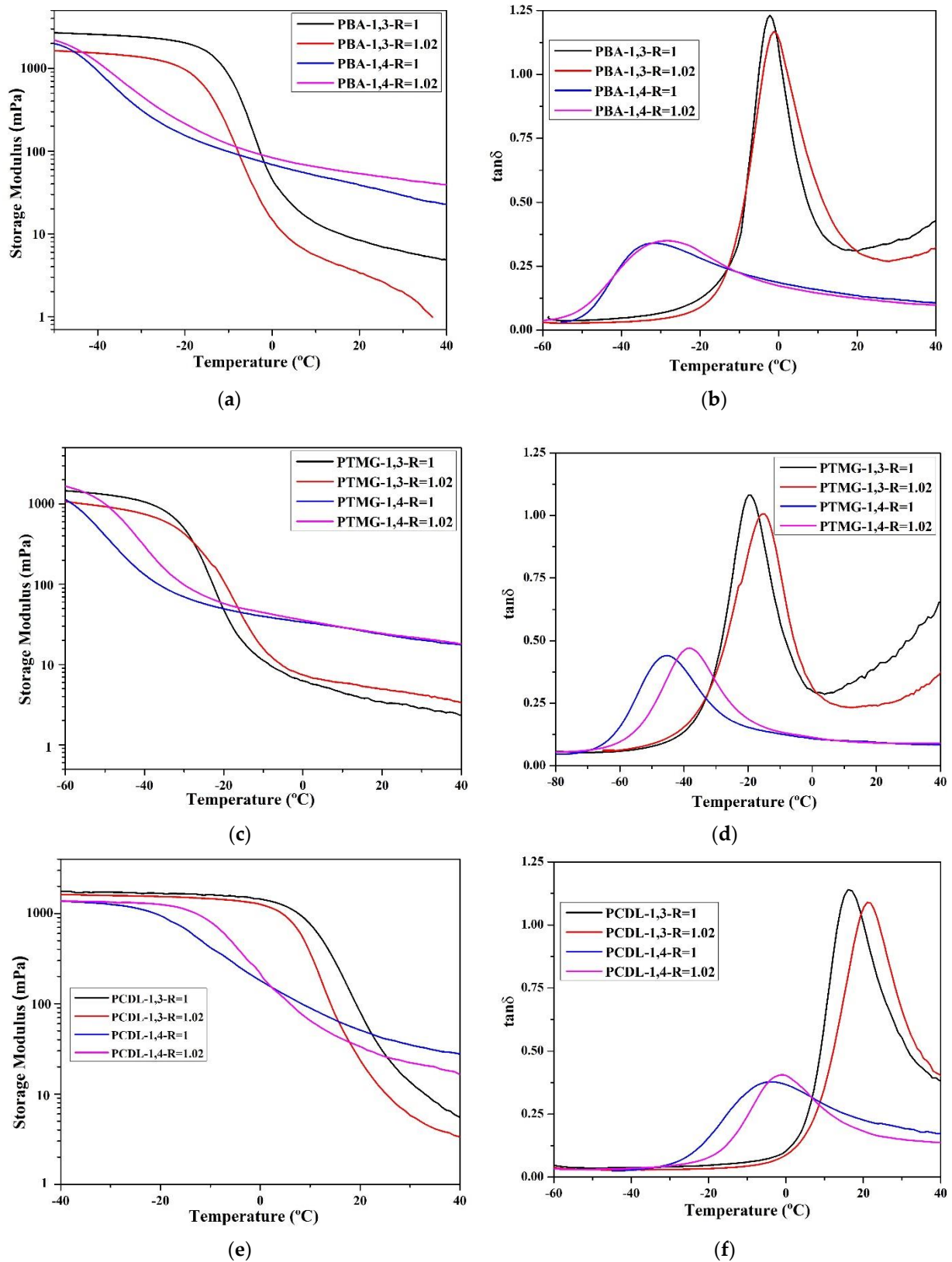


Figure 4. According to dynamic mechanical analysis (DMA), the following parameters were measured: storage modulus (mPa) and $\tan \delta$ related to the temperature rate; storage modulus (a) and $\tan \delta$ (b) of TPU from PBA, storage modulus (c) and $\tan \delta$ (d) of TPU from PTMG; storage modulus (e) and $\tan \delta$ (f) of TPU from PCDL.

All the glass transition point (T_g) data obtained through DMA analysis are listed in Table 4. The T_g of TPU synthesized using 1,3-BDO was approximately 10–15 °C higher than the T_g of TPU synthesized using 1,4-BDO. The reason behind this is that 1,3-BDO contains a methyl group in its structure, and this results in an asymmetrical TPU structure during the polymerization process. The DMA results also confirmed that TPU synthesized using 1,3-BDO has viscoelasticity (this must correspond with the conclusion from the DSC scan, which tends to be viscous materials). The storage modulus (G') data confirmed that TPUs synthesized using 1,3-BDO have greater viscoelasticity than TPUs synthesized using 1,4-BDO.

Table 4. The $\tan \delta$ crest peak location on the DMA spectrum was used as the glass transition temperature (T_g). Relevant numerical values associated with TPU prepared through the polymerization of different butanediols with different R values.

Chain Extender [NCO]/[OH] (R Value)	1,3-BDO		1,4-BDO	
	1.00	1.02	1.00	1.02
PBA-1000	−2.8 °C	−1.2 °C	−31.3 °C	−28.3 °C
PCDL-1000	8.1 °C	10.6 °C	−3.5 °C	−1.3 °C
PTMG-1000	−19.1 °C	−13.9 °C	−44.9 °C	−38.4 °C

Next, AFM was used to identify the microphase distribution of the TPUs. The surfaces of TPUs that were subjected to thermal processing and those not subjected to thermal processing were analyzed to confirm their phase separation condition and structure. The annealing was conducted at 100 °C. With the increase of annealing time, changes in the crystal could be evaluated. All the captured images were uniformly modified to the same scale for direct comparison. Figure 5 presents the AFM images of TPUs synthesized from PBA and PTMG; the images clearly indicate that obvious microphase separation was present in TPUs synthesized using 1,3-BDO. Because the miscibility between the hard and soft chain segments is poor, the differentiation between the dark and light zones is fairly apparent. After being subjected to 10 and 20 h of thermal processing, only the dark-colored aggregates increased substantially. According to the surface structure, the crystals aggregated with the increase of thermal processing time. AFM images of thermal treatment were presented in Figure S1 for TPU composed by PBA and Figure S3 for TPU composed by PTMG. The increase in the number of TPU hard chain segments resulted in the formation of more crystals, which in turn led to more aggregates. The AFM scanned images of TPUs with disparate R value were presented in Figure S2 for TPU synthesized from PBA, and Figure S4 for TPU synthesized from PTMG to address the results of aggregation.

Compared with the AFM images of TPUs synthesized with PCDL, the constituents of TPUs synthesized with PBA and PTMG are slightly different; the AFM images indicate that regardless of whether TPUs were synthesized using 1,4-BDO or 1,3-BDO, the aggregate of crystals was present in both types of TPU. The aggregate condition of the two types of TPU is depicted in Figure 6; TPUs synthesized using 1,3-BDO as a chain extender exhibit a more obvious phase separation phenomenon. It has the same phenomenon that more aggregates with the increase of the hard phase presented in Figures S5 and S6.

In all the synthesized TPU series, an increase in hardness resulted in an increase of crystallization. The microphase separation of the TPUs synthesized using PCDL revealed that regardless of whether the TPUs were synthesized using 1,3-BDO or 1,4-BDO, the aggregation of crystallizations was readily observable in the synthesized products; this is because the polarized structure of polycarbonate bonds is beneficial for the production of hard chains [48].

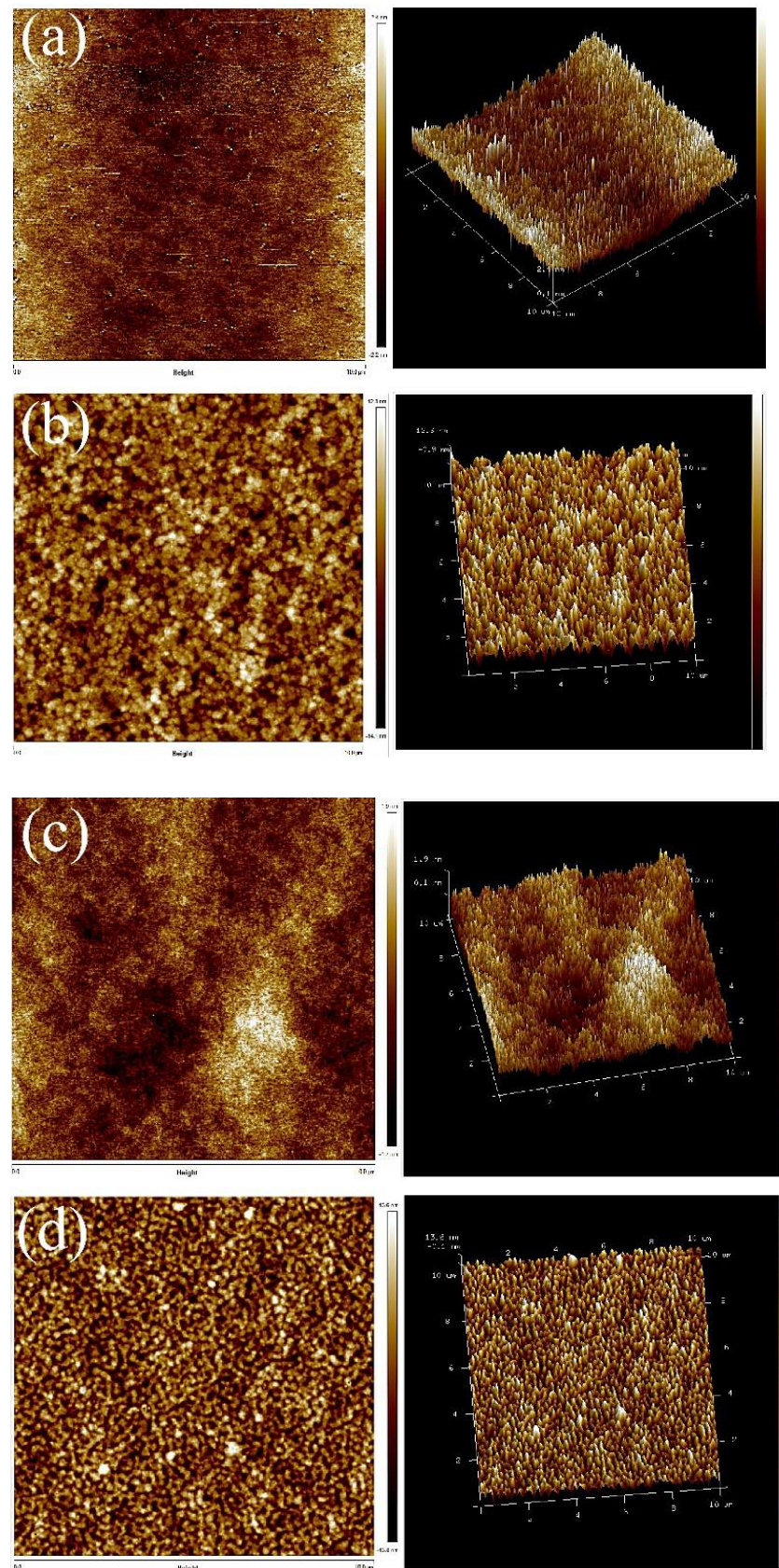


Figure 5. Atomic force microscope (AFM) scanned images: (a) PBA-1,3-BDO, (b) PBA-1,4-BDO, (c) PTMG-1,3-BDO, (d) PTMG-1,4-BDO.

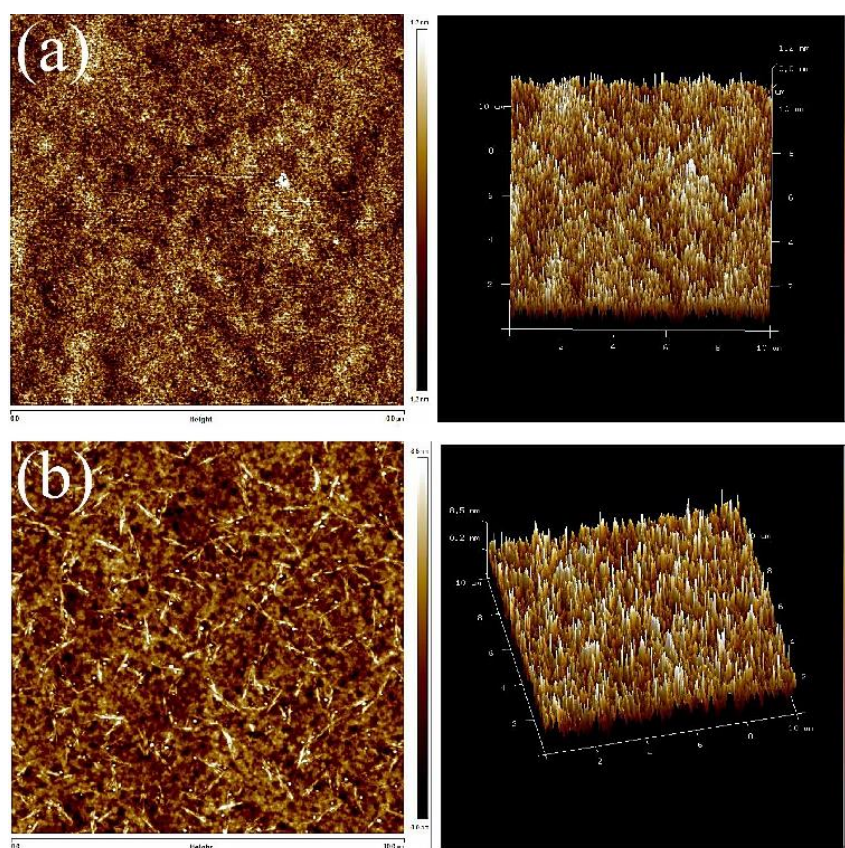


Figure 6. AFM scanned images: (a) PCDL-1,3-BDO, (b) PCDL-1,4-BDO.

Next, the researchers performed a rheological analysis using two methods to understand the shear-thinning behaviors via frequency sweep and the viscoelastic characteristics under the oscillatory mode; the shear-thinning data related to the shear rate are presented in Figure 7. The results indicate that for the PBA and the PTMG groups, the melt viscosity of TPUs synthesized using 1,4-BDO was higher than the melt viscosity of TPUs synthesized using 1,3-BDO. For the PCDL, TPU synthesized using 1,4-BDO or 1,3-BDO as the chain extender had a similar shear-thinning curve. Looking at the morphological analysis conducted using AFM, we can explain this property by referring to the influence of structure. Regardless of the type of butanediol used to synthesize the PCDL, the aggregation of the soft and hard chain zones would be more even and compatible than in the other groups. The higher level of microphase compatibility would result in a satisfactory level of melt viscosity obtained from the flow behavior.

Next, to confirm the viscoelasticity, a vibration scan experiment was performed at 200 °C. The data are compiled and displayed in Figure 8. A vibration rheology experiment allows rapid observation of the presence of an intersection point between G' and G'' . The loss modulus (G'') of all the TPUs was higher than their storage modulus (G'); this indicates all the TPU fused masses are viscous and can be used as hot melt adhesive. A difference between G' and G'' could also be detected; the difference between G' and G'' was larger in two groups, namely PBA and PTMG. TPU polymerized using 1,3-BDO has a more loosely organized internal structure; thus, the maintenance of a crystal structure is more difficult. Relatively, for TPUs polymerized using PCDL, differences between TPUs synthesized using different types of butanediol are minor. They have a similar internal structure, and their microphase compatibility is relatively better. Thus, they could be candidate materials for hot melt adhesives [9].

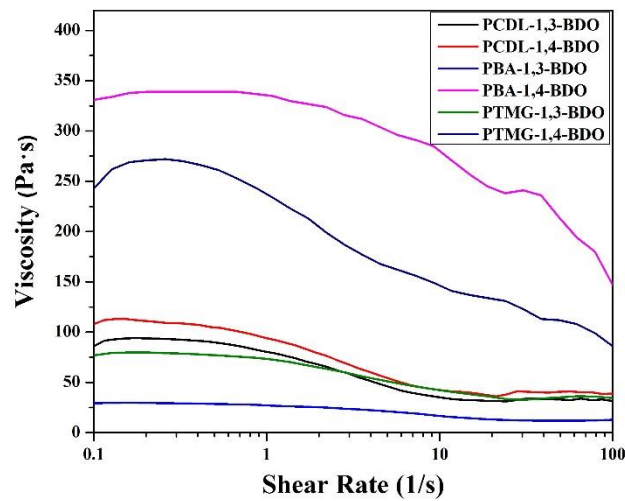


Figure 7. Shear thinning characteristics of TPUs produced by applying 1,3-BDO or 1,4-BDO during the synthesizing of PBA, PTMG, or PCDL.

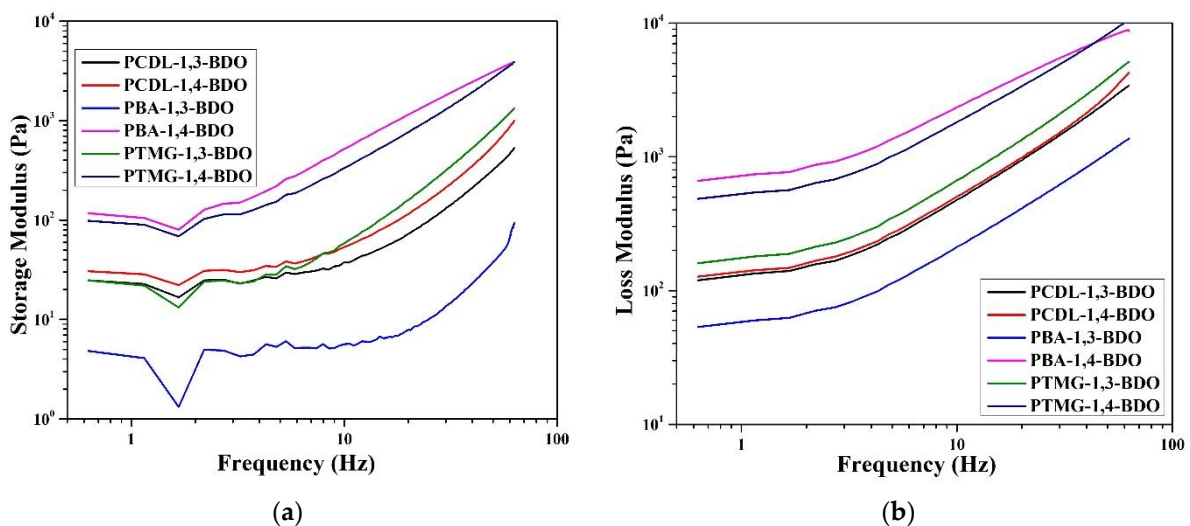


Figure 8. Rheological properties. (a) Storage modulus and (b) loss modulus of TPUs prepared using 1,3-BDO or 1,4-BDO during the synthesizing of PBA, PTMG, or PCDL.

4. Conclusions

Modified TPUs, with different chain extenders, can be prepared using the one-shot solvent-free bulk polymerization method. Examination of their structures, thermal properties, morphology, and rheological properties revealed that the changing of chain extenders did not affect the structure of the main polymer chain segments; this was also applicable to the synthesizing of high molecular polymers. FT-IR results indicated that the two are structurally similar. Thermal analysis performed using DSC and DMA revealed that the T_g of TPUs prepared using 1,3-BDO as the chain extender was approximately 10–15 °C higher than that of the TPUs prepared using 1,4-BDO as the chain extender. The main reason was that rotation difficulties in the branched chain structure resulted in an increase of T_g . Additionally, the T_g point would also slightly increase, by 1 to 2 °C, with the increase in the TPU's hard chain segment. The DSC scanning data also revealed that the T_m of TPU made with 1,3-BDO belongs to the category of amorphous materials; the DMA testing spectrum revealed that a TPU containing 1,3-BDO exhibits the characteristic of viscoelasticity. The

differences in the thermal properties results prompted the researchers to perform further study on the viscoelastic and rheological properties.

Subsequently, investigations related to morphological analysis and rheological measurement were conducted. Detailed morphological analysis was performed using AFM scanning. In PBA and PTMG, TPUs that contained 1,3-BDO exhibited an obvious microphase separation, which was a clear difference between hard and soft zones; the separation phenomenon did not change even when the hard chain content was increased. However, in the PCDL group, the microphase separation was not obvious; we believe that the reason for this is that the polycarbonate bonds in PCDL have excellent stiffness, which could help maintain structural stability. The results of the rheological measurements (to examine the viscoelasticity behavior) were similar to those obtained using the morphological test. For PBA and PTMG groups, TPUs that contained 1,3-BDO had poor viscoelasticity. The rheological results clearly confirmed that for PCDL, even when 1,3-BDO was employed as a chain extender during the synthesizing process, the TPUs synthesized were similar to the TPUs synthesized using 1,4-BDO as a chain extender; the reason behind this is that PCDL has a side methyl group, resulting in a high free volume rotation obstacle—thus, the increase of T_g . In addition, T_g range of the TPUs synthesized using PCDL is within room temperature (15–20 °C). Another factor is that the carbonate group of the PCDL structure contains three oxygen atoms with the six lone pairs of electrons that will mutually repel each other; this causes the compatibility of TPUs synthesized using PCDL to be better than that of the TPUs synthesized using polyester or polyether. The conclusions of this study indicate that PCDL could be used in conjunction with 1,3-BDO as a candidate material for future smart material development.

Supplementary Materials: The following are available online at <https://www.mdpi.com/2076-3417/11/2/698/s1>, Figure S1: AFM image of (A) PBA-1,3-R = 1 at 0 h (C) PBA-1,3-R = 1 after 10 h (E) PBA-1,3-R = 1 after 20 h. (B) PBA-1,4-R = 1 at 0 h (D) PBA-1,4-R = 1 after 10 h (F) PBA-1,4-R = 1 after 20 h., Figure S2: AFM image of (A) PBA-1,3-R = 1.02 at 0 h (C) PBA-1,3-R = 1.02 after 10 h (E) PBA-1,3-R = 1.02 after 20 h. (B) PBA-1,4-R = 1.02 at 0 h (D) PBA-1,4-R = 1.02 after 10 h (F) PBA-1,4-R = 1.02 after 20 h., Figure S3: AFM image of (A) PTMG-1,3-R = 1 at 0 h (C) PTMG-1,3-R = 1 after 10 h (E) PTMG-1,3-R = 1 after 20 hr. (B) PTMG-1,4-R = 1 at 0 h (D) PTMG-1,4-R = 1 after 10 h (F) PTMG-1,4-R = 1 after 20 h., Figure S4: AFM image of (A) PTMG-1,3-R = 1.02 at 0 h (C) PTMG-1,3-R = 1.02 after 10 h (E) PTMG -1,3-R = 1.02 after 20 hr. (B) PTMG -1,4-R = 1.02 at 0 h (D) PTMG -1,4-R = 1.02 after 10 h (F) PTMG -1,4-R = 1.02 after 20 h., Figure S5: AFM image of (A) PCDL-1,3-R = 1 at 0 h (C) PCDL-1,3-R = 1 after 10 h (E) PCDL -1,3-R = 1 after 20 hr. (B) PCDL-1,4-R = 1 at 0 h (D) PCDL-1,4-R = 1 after 10 h (F) PCDL -1,4-R = 1 after 20 h., Figure S6: AFM image of (A) PCDL-1,3-R = 1.02 at 0 h (C) PCDL-1,3-R = 1.02 after 10 h (E) PCDL -1,3-R = 1.02 after 20 hr. (B) PCDL-1,4-R = 1.02 at 0 h (D) PCDL-1,4-R = 1.02 after 10 h (F) PCDL -1,4-R = 1.02 after 20 h.

Author Contributions: Conceptualization, C.-F.L.; Data curation, C.-F.L.; Formal analysis, C.-F.L. and C.-W.C.; Funding acquisition, S.-P.R.; Investigation, C.-F.L., C.-W.C. and F.-S.C.; Methodology, C.-W.C. and F.-S.C.; Supervision, S.-P.R.; Writing—original draft, C.-F.L.; Writing—review and editing, C.-F.L. and C.-W.C. All authors have read and agreed to the published version of the manuscript.

Funding: This research was funded by the Ministry of Science and Technology of Taiwan, grant number MOST 109-2634-F-027-001-.

Institutional Review Board Statement: Not applicable.

Informed Consent Statement: Not applicable.

Data Availability Statement: Data is contained within the article.

Conflicts of Interest: The authors declare no conflict of interest.

References

1. Datta, J.; Kasprzyk, P. Thermoplastic polyurethanes derived from petrochemical or renewable resources: A comprehensive review. *Polym. Eng. Sci.* **2018**, *58*, E14–E35. [[CrossRef](#)]
2. Queiroz, A.U.B.; Collares-Queiroz, F.P. Innovation and Industrial Trends in Bioplastics. *Polym. Rev.* **2009**, *49*, 65–78. [[CrossRef](#)]
3. Engels, H.-W.; Pirkel, H.-G.; Albers, R.; Albach, R.W.; Krause, J.; Hoffmann, A.; Casselmann, H.; Dormish, J. Polyurethanes: Versatile Materials and Sustainable Problem Solvers for Today's Challenges. *Angew. Chem. Int. Ed.* **2013**, *52*, 9422–9441. [[CrossRef](#)] [[PubMed](#)]
4. Jofre-Reche, J.A.; García-Pacios, V.; Costa, V.; Colera, M.; Martín-Martínez, J.M. Role of the interactions between carbonate groups on the phase separation and properties of waterborne polyurethane dispersions prepared with copolymers of polycarbonate diol. *Prog. Org. Coat.* **2015**, *88*, 199–211. [[CrossRef](#)]
5. Liu, R.; Dai, H.; Zhou, Q.; Zhang, Q.; Zhang, P. Synthesis and characterization of shape-memory poly carbonate urethane microspheres for future vascular embolization. *J. Biomater. Sci. Polym. Ed.* **2016**, *27*, 1248–1261. [[CrossRef](#)] [[PubMed](#)]
6. Wang, J.; Zhang, H.; Miao, Y.; Qiao, L.; Wang, X.; Wang, F. Waterborne polyurethanes from CO₂ based polyols with comprehensive hydrolysis/oxidation resistance. *Green Chem.* **2016**, *18*, 524–530. [[CrossRef](#)]
7. Wang, J.; Zhang, H.; Miao, Y.; Qiao, L.; Wang, X.; Wang, F. UV-curable waterborne polyurethane from CO₂-polyol with high hydrolysis resistance. *Polymer* **2016**, *100*, 219–226. [[CrossRef](#)]
8. Brannigan, R.P.; Dove, A.P. Synthesis, properties and biomedical applications of hydrolytically degradable materials based on aliphatic polyesters and polycarbonates. *Biomater. Sci.* **2017**, *5*, 9–21. [[CrossRef](#)]
9. Orgilés-Calpena, E.; Arán-Aís, F.; Torró-Palau, A.M.; Orgilés-Barceló, C. Novel polyurethane reactive hot melt adhesives based on polycarbonate polyols derived from CO₂ for the footwear industry. *Int. J. Adhes. Adhes.* **2016**, *70*, 218–224. [[CrossRef](#)]
10. Kumagai, S.; Motokucho, S.; Yabuki, R.; Anzai, A.; Kameda, T.; Watanabe, A.; Nakatani, H.; Yoshioka, T. Effects of hard- and soft-segment composition on pyrolysis characteristics of MDI, BD, and PTMG-based polyurethane elastomers. *J. Anal. Appl. Pyrolysis* **2017**, *126*, 337–345. [[CrossRef](#)]
11. Korley, L.T.J.; Pate, B.D.; Thomas, E.L.; Hammond, P.T. Effect of the degree of soft and hard segment ordering on the morphology and mechanical behavior of semicrystalline segmented polyurethanes. *Polymer* **2006**, *47*, 3073–3082. [[CrossRef](#)]
12. Christenson, C.P.; Harthcock, M.A.; Meadows, M.D.; Spell, H.L.; Howard, W.L.; Creswick, M.W.; Guerra, R.E.; Turner, R.B. Model MDI/butanediol polyurethanes: Molecular structure, morphology, physical and mechanical properties. *J. Polym. Sci. Part B Polym. Phys.* **1986**, *24*, 1401–1439. [[CrossRef](#)]
13. Pattamaprom, C.; Wu, C.-H.; Chen, P.-H.; Huang, Y.-L.; Ranganathan, P.; Rwei, S.-P.; Chuan, F.-S. Solvent-Free One-Shot Synthesis of Thermoplastic Polyurethane Based on Bio-Poly(1,3-propylene succinate) Glycol with Temperature-Sensitive Shape Memory Behavior. *ACS Omega* **2020**, *5*, 4058–4066. [[CrossRef](#)] [[PubMed](#)]
14. Yang, B.; Huang, W.M.; Li, C.; Lee, C.M.; Li, L. On the effects of moisture in a polyurethane shape memory polymer. *Smart Mater. Struct.* **2004**, *13*, 191–195. [[CrossRef](#)]
15. Kim, S.-M.; Jeon, H.; Shin, S.-H.; Park, S.-A.; Jegal, J.; Hwang, S.Y.; Oh, D.X.; Park, J. Superior Toughness and Fast Self-Healing at Room Temperature Engineered by Transparent Elastomers. *Adv. Mater.* **2018**, *30*, 1705145. [[CrossRef](#)] [[PubMed](#)]
16. Xie, T. Recent advances in polymer shape memory. *Polymer* **2011**, *52*, 4985–5000. [[CrossRef](#)]
17. Hu, J.; Zhu, Y.; Huang, H.; Lu, J. Recent advances in shape-memory polymers: Structure, mechanism, functionality, modeling and applications. *Prog. Polym. Sci.* **2012**, *37*, 1720–1763. [[CrossRef](#)]
18. Thakur, S. Shape Memory Polymers for Smart Textile Applications. In *Textiles for Advanced Applications*; Kumar, B., Thakur, S., Eds.; IntechOpen: Croatia, Croatia, 2017. [[CrossRef](#)]
19. Blackwell, J.; Gardner, K.H. Structure of the hard segments in polyurethane elastomers. *Polymer* **1979**, *20*, 13–17. [[CrossRef](#)]
20. Sonnenschein, M.F.; Lysenko, Z.; Brune, D.A.; Wendt, B.L.; Schrock, A.K. Enhancing polyurethane properties via soft segment crystallization. *Polymer* **2005**, *46*, 10158–10166. [[CrossRef](#)]
21. Hood, M.A.; Wang, B.; Sands, J.M.; La Scala, J.J.; Beyer, F.L.; Li, C.Y. Morphology control of segmented polyurethanes by crystallization of hard and soft segments. *Polymer* **2010**, *51*, 2191–2198. [[CrossRef](#)]
22. Sheikhy, H.; Shahidzadeh, M.; Ramezanzadeh, B.; Noroozi, F. Studying the effects of chain extenders chemical structures on the adhesion and mechanical properties of a polyurethane adhesive. *J. Ind. Eng. Chem.* **2013**, *19*, 1949–1955. [[CrossRef](#)]
23. Xie, F.; Zhang, T.; Bryant, P.; Kurusingal, V.; Colwell, J.M.; Laycock, B. Degradation and stabilization of polyurethane elastomers. *Prog. Polym. Sci.* **2019**, *90*, 211–268. [[CrossRef](#)]
24. Zvosec, D.L.; Smith, S.W.; McCutcheon, J.R.; Spillane, J.; Hall, B.J.; Peacock, E.A. Adverse Events, Including Death, Associated with the Use of 1,4-Butanediol. *N. Engl. J. Med.* **2001**, *344*, 87–94. [[CrossRef](#)] [[PubMed](#)]
25. Lora-Tamayo, C.; Tena, T.; Rodríguez, A.; Sancho, J.R.; Molina, E. Intoxication due to 1,4-butanediol. *Forensic Sci. Int.* **2003**, *133*, 256–259. [[CrossRef](#)]
26. Jiang, Y.; Liu, W.; Zou, H.; Cheng, T.; Tian, N.; Xian, M. Microbial production of short chain diols. *Microb. Cell Fact.* **2014**, *13*, 165. [[CrossRef](#)] [[PubMed](#)]
27. Zhang, Y.; Liu, D.; Chen, Z. Production of C₂–C₄ diols from renewable bioresources: New metabolic pathways and metabolic engineering strategies. *Biotechnol. Biofuels* **2017**, *10*, 299. [[CrossRef](#)] [[PubMed](#)]
28. Zhang, L.; Huang, M.; Yu, R.; Huang, J.; Dong, X.; Zhang, R.; Zhu, J. Bio-based shape memory polyurethanes (Bio-SMPUs) with short side chains in the soft segment. *J. Mater. Chem. A* **2014**, *2*, 11490–11498. [[CrossRef](#)]

29. Gopakumar, S.; Gopinathan Nair, M.R. Determination of molecular parameters of NR/PU block copolymers by transport studies. *Eur. Polym. J.* **2005**, *41*, 2002–2009. [[CrossRef](#)]
30. Paul, C.J.; Gopinathan Nair, M.R.; Neelakantan, N.R.; Koshy, P.; Idage, B.B.; Bhelhekar, A.A. Segmented block copolymers of natural rubber and 1, 3-butanediol–toluene diisocyanate oligomers. *Polymer* **1998**, *39*, 6861–6874. [[CrossRef](#)]
31. Radhakrishnan Nair, M.N.; Gopinathan Nair, M.R. Studies on impact modification and fractography of solution cast blends of PVC and NR/PU block copolymers. *Polym. Bull.* **2012**, *68*, 859–877. [[CrossRef](#)]
32. Makshina, E.V.; Dusselier, M.; Janssens, W.; Degreève, J.; Jacobs, P.A.; Sels, B.F. Review of old chemistry and new catalytic advances in the on-purpose synthesis of butadiene. *Chem. Soc. Rev.* **2014**, *43*, 7917–7953. [[CrossRef](#)] [[PubMed](#)]
33. Xu, W.J.; Wang, J.J.; Zhang, S.Y.; Sun, J.; Qin, C.X.; Dai, L.X. Tuning chain extender structure to prepare high-performance thermoplastic polyurethane elastomers. *RSC Adv.* **2018**, *8*, 20701–20711. [[CrossRef](#)]
34. Datta, J.; Głowińska, E. Effect of hydroxylated soybean oil and bio-based propanediol on the structure and thermal properties of synthesized bio-polyurethanes. *Ind. Crop. Prod.* **2014**, *61*, 84–91. [[CrossRef](#)]
35. Lei, W.; Fang, C.; Zhou, X.; Cheng, Y.; Yang, R.; Liu, D. Morphology and thermal properties of polyurethane elastomer based on representative structural chain extenders. *Thermochim. Acta* **2017**, *653*, 116–125. [[CrossRef](#)]
36. Kim, J.-H.; Kim, J.-R.; Ahn, C.-H. Novel biobased copolyesters based on 1,2-propanediol or 2,3-butanediol with the same ethylene skeletal structure as PETG. *Polymer* **2018**, *135*, 314–326. [[CrossRef](#)]
37. Debuissy, T.; Sangwan, P.; Pollet, E.; Avérous, L. Study on the structure-properties relationship of biodegradable and biobased aliphatic copolyesters based on 1,3-propanediol, 1,4-butanediol, succinic and adipic acids. *Polymer* **2017**, *122*, 105–116. [[CrossRef](#)]
38. Nair, M.N.R.; Nair, M.R.G. Synthesis and characterisation of soluble block copolymers from NR and TDI based polyurethanes. *J. Mater. Sci.* **2008**, *43*, 738–747. [[CrossRef](#)]
39. Debuissy, T.; Pollet, E.; Avérous, L. Synthesis of potentially biobased copolyesters based on adipic acid and butanediols: Kinetic study between 1,4- and 2,3-butanediol and their influence on crystallization and thermal properties. *Polymer* **2016**, *99*, 204–213. [[CrossRef](#)]
40. Schrock, A.K.; Hamilton, H.S.; Johnson, N.D.; Del Rosario, C.; Thompson, B.; Ulrich, K.; Coggio, W.D. Thermal characterization and crystallization kinetics of polyester polyols derived from adipic acid and bio-based succinic acid with 1,4-butanediol and 1,6-hexanediol. *Polymer* **2016**, *101*, 233–240. [[CrossRef](#)]
41. Rashmi, B.J.; Rusu, D.; Prashantha, K.; Lacrampe, M.-F.; Krawczak, P. Development of bio-based thermoplastic polyurethanes formulations using corn-derived chain extender for reactive rotational molding. *Express Polym. Lett.* **2013**, *7*, 852–862. [[CrossRef](#)]
42. Pedrazzoli, D.; Manas-Zloczower, I. Understanding phase separation and morphology in thermoplastic polyurethanes nanocomposites. *Polymer* **2016**, *90*, 256–263. [[CrossRef](#)]
43. Jiang, L.; Wu, J.; Nedolisa, C.; Saiani, A.; Assender, H.E. Phase Separation and Crystallization in High Hard Block Content Polyurethane Thin Films. *Macromolecules* **2015**, *48*, 5358–5366. [[CrossRef](#)]
44. Yilgör, I.; Yilgör, E.; Wilkes, G.L. Critical parameters in designing segmented polyurethanes and their effect on morphology and properties: A comprehensive review. *Polymer* **2015**, *58*, A1–A36. [[CrossRef](#)]
45. Xiao, Y.; Jiang, L.; Liu, Z.; Yuan, Y.; Yan, P.; Zhou, C.; Lei, J. Effect of phase separation on the crystallization of soft segments of green waterborne polyurethanes. *Polym. Test.* **2017**, *60*, 160–165. [[CrossRef](#)]
46. Cao, Q.; Cai, Y.; Jing, B.; Liu, P. Structure and mechanical properties of thermoplastic polyurethane, based on hyperbranched polyesters. *J. Appl. Polym. Sci.* **2006**, *102*, 5266–5273. [[CrossRef](#)]
47. Niemczyk, A.; Piegat, A.; Sonseca Olalla, Á.; El Fray, M. New approach to evaluate microphase separation in segmented polyurethanes containing carbonate macrodiol. *Eur. Polym. J.* **2017**, *93*, 182–191. [[CrossRef](#)]
48. Xiao, S.; Hossain, M.M.; Liu, P.; Wang, H.; Hu, F.; Sue, H.-J. Scratch behavior of model polyurethane elastomers containing different soft segment types. *Mater. Des.* **2017**, *132*, 419–429. [[CrossRef](#)]
49. De León, A.S.; Domínguez-Calvo, A.; Molina, S.I. Materials with enhanced adhesive properties based on acrylonitrile-butadiene-styrene (ABS)/thermoplastic polyurethane (TPU) blends for fused filament fabrication (FFF). *Mater. Des.* **2019**, *182*, 108044. [[CrossRef](#)]
50. Ruan, M.; Luan, H.; Wang, G.; Shen, M. Bio-polyols synthesized from bio-based 1,3-propanediol and applications on polyurethane reactive hot melt adhesives. *Ind. Crop. Prod.* **2019**, *128*, 436–444. [[CrossRef](#)]
51. Pan, X.; Zeng, Z.; Xue, W.; Zhu, W. Hot melt adhesive properties of PA/TPU blends compatibilized by EVA-g-MAH. *J. Adhes. Sci. Technol.* **2017**, *31*, 943–957. [[CrossRef](#)]
52. Wang, S.; Liu, Z.; Zhang, L.; Guo, Y.; Song, J.; Lou, J.; Guan, Q.; He, C.; You, Z. Strong, detachable, and self-healing dynamic crosslinked hot melt polyurethane adhesive. *Mater. Chem. Front.* **2019**, *3*, 1833–1839. [[CrossRef](#)]
53. Tous, L.; Ruseckaite, R.A.; Ciannamea, E.M. Sustainable hot-melt adhesives based on soybean protein isolate and polycaprolactone. *Ind. Crop. Prod.* **2019**, *135*, 153–158. [[CrossRef](#)]
54. Orgilés-Calpena, E.; Arán-Aís, F.; Torró-Palau, A.M.; Montiel-Parreño, E.; Orgilés-Barceló, C. Synthesis of polyurethanes from CO₂-based polyols: A challenge for sustainable adhesives. *Int. J. Adhes. Adhes.* **2016**, *67*, 63–68. [[CrossRef](#)]
55. Fuensanta, M.; Martín-Martínez, J.M. Thermoplastic polyurethane pressure sensitive adhesives made with mixtures of polypropylene glycols of different molecular weights. *Int. J. Adhes. Adhes.* **2019**, *88*, 81–90. [[CrossRef](#)]
56. Fuensanta, M.; Martín-Martínez, J.M. Thermoplastic polyurethane coatings made with mixtures of polyethers of different molecular weights with pressure sensitive adhesion property. *Prog. Org. Coat.* **2018**, *118*, 148–156. [[CrossRef](#)]

57. Wamuo, O.; Wu, Y.; Hsu, S.L.; Paul, C.W.; Eodice, A.; Huang, K.-Y.; Chen, M.-H.; Chang, Y.-H.; Lin, J.-L. Effects of chain configuration on the crystallization behavior of polypropylene based copolymers. *Polymer* **2017**, *116*, 342–349. [[CrossRef](#)]
58. Bajsic, E.G.I.; Rek, V. Thermal stability of polyurethane elastomers before and after UV irradiation n.d.:10. *J. Appl. Polym. Sci.* **2001**, *79*, 864–873. [[CrossRef](#)]
59. Chen, S.; Wang, Q.; Wang, T. Preparation, tensile, damping and thermal properties of polyurethanes based on various structural polymer polyols: Effects of composition and isocyanate index. *J. Polym. Res.* **2012**, *19*, 9994. [[CrossRef](#)]
60. Cipriani, E.; Zanetti, M.; Brunella, V.; Costa, L.; Bracco, P. Thermoplastic polyurethanes with polycarbonate soft phase: Effect of thermal treatment on phase morphology. *Polym. Degrad. Stab.* **2012**, *97*, 1794–1800. [[CrossRef](#)]
61. Meng, Q.; Hu, J. A review of shape memory polymer composites and blends. *Compos. Part A Appl. Sci. Manuf.* **2009**, *40*, 1661–1672. [[CrossRef](#)]